Chromospheric activity in several single late-type stars

2015 Res. Astron. Astrophys. 15 252

(http://iopscience.iop.org/1674-4527/15/2/009)

RAA 2015 Vol. **15** No. **2**, 252–274 doi: 10.1088/1674–4527/15/2/009
http://www.raa-journal.org *http://www.iop.org/journals/raa*

Research in Astronomy and Astrophysics

Chromospheric activity in several single late-type stars *

Li-Yun Zhang[1,2], Qing-Feng Pi[1] and Zhong-Zhong Zhu[1]

[1] Department of Physics & NAOC-GZU Sponsored Center for Astronomy Research, College of Science, Guizhou University, Guiyang 550025, China; *Liy_zhang@hotmail.com*
[2] Guizhou Province Big Data Industry Development Application Research Institute, Guizhou University, Guiyang 550025, China

Received 2014 January 24; accepted 2014 June 3

Abstract New high-resolution echelle spectra of six single late-type Pleiades-like stars (V368 Cep, EP Eri, DX Leo, GJ 211, PW And and V383 Lac) were obtained with the 2.16 meter telescope at Xinglong Station in 2008–2010. Using the spectral subtraction technique, we analyzed our spectroscopic data and calculated the equivalent widths of excess emission from several indicators of chromospheric activity (Na I D_1, D_2, Hα and Ca II infrared triplet lines). All our results using chromospheric activity indicators confirmed the previous findings. In addition, the maximum amplitudes of chromospheric rotational modulation and the ratio of EW_{8542}/EW_{8498} were found to rise with increasing $v \sin i$ velocity.

Key words: stars: chromospheres — stars: spectroscopic — stars: activity — stars: rotation — late-type

1 INTRODUCTION

Late-type stars with thick convective zones and rapid rotation exhibit phenomena related to magnetic activity, such as starspots, plages and flares (Berdyugina 2005; Güdel 2002; Hall 2008; Strassmeier 2009; Gu et al. 2002). However, in many of these kinds of stars, the details related to active phenomena are not well understood and need to be studied, especially properties of their chromospheric activity (Wang et al. 2009; Zhao et al. 2011, 2013), chromospheric rotational modulation and magnetic cycle (Baliunas et al. 1995; etc). To understand stellar chromospheric activities, herein we study the magnetic activities of late-type stars with different stellar parameters by using high-resolution spectroscopy, and investigate the properties of magnetic activity in their chromosphere, and relations between chromospheric activity and stellar parameters (Zhang 2011).

Chromospheric activity is a proxy for levels of variable activity in late-type stars. The spectral subtraction technique has been widely used to discuss chromospheric activity by observing several optical lines: the Ca II H & K, He I D_3, Na I D_1, D_2, Hα, Hβ and Ca II infrared triplet (IRT) lines (Barden 1985; Fekel et al. 1986; Gunn & Doyle 1997; Lazaro & Arevalo 1997; Montes et al. 2000; Frasca et al. 2002; Griffin & Griffin 2004; Gálvez et al. 2009; Frasca et al. 2010; Cao & Gu 2012; Zhang et al. 2014; etc). Because chromospheric activities are mostly variable with time and phase

* Supported by the National Natural Science Foundation of China.

(Baliunas et al. 1995), we need more data to calculate their average values to obtain the precise relationship between chromospheric activity and stellar parameters.

In this paper, we describe our spectroscopic studies of six targets that resemble single late-type stars seen in the Pleiades with a spectral type similar to K0-2 V. First, we introduce new high-resolution optical observations. After that, we intend to discuss the chromospheric activity indicators and diagnostic technique. Then, we discuss the behavior of chromospheric activity, and the relationship between chromospheric activity and stellar rotation.

First, we introduce new high-resolution optical observations in Section 2. After that, we intend to discuss the chromospheric activity indicators and diagnostic technique in Section 3. Then, we discuss the behavior of the chromospheric activity in Sections 4 and 5, and the relationship between chromospheric activity and stellar rotation in Section 6.

2 OBSERVATIONS AND REDUCTIONS

Our high-resolution spectroscopic observations of V368 Cep, EP Eri, DX Leo, GJ 211, PW And and V383 Lac (see Table 1) were made using the 2.16 m telescope at Xinglong Station, administered by National Astronomical Observatories, Chinese Academy of Sciences, in five observing sessions: 2008 September 19; 2009 November 1 and December 29–31; and 2010 January 2–4 and February 2–4. In our five observing sessions, we obtained a total of 30 spectra. The spectral resolution of the Coudé echelle spectrograph is about 37 000 with a spectral range of 5600–9100 Å (Zhao & Li 2001). The reciprocal dispersions and spectral resolution for the region with various chromospheric activity indictors were listed in a previous paper (Zhang & Gu 2008). At the same time, we also observed several inactive stars (HR 222 (K2.5 V), HR 166 (K0 V), HR 1614 (K3 V), GJ 706 (K2 V) and HD 3765 (K2 V)) with spectral types and luminosity classes close to our objects in order to construct synthesized spectra.

Table 1 Stellar Parameters of Our Selected Single Late-Type Stars

Name	HD/BD	Spectral type	$V-R$	$B-V$	$v \sin i$ ($\mathrm{km\ s^{-1}}$)	Orbital period (d)
PW And	HD 1405	K2 V	0.74	1	23.4	1.75
V383 Lac	BD +48 3686	K1 V	0.69	0.83	19.8	2.42
V368 Cep	HD 220140	K1 V	0.61	0.87	16.1	2.74
DX Leo	HD 82443	K0 V	0.64	0.78	6.2	5.38
EP Eri	HD 17925	K1 V	0.69	0.86	6.2	6.85
GJ 211	HD 37394	K1 V	0.69	0.84	4.0	10.9

References: Montes et al. (2001a); Høg et al. (2000).

We reduced our spectra using the IRAF package that includes zero subtraction, flat field division, background subtraction, cosmic-ray removal and extraction of 1D spectra. The wavelengths were calibrated by the spectrum from a Th-Ar lamp. Then, the observed spectra were normalized by a polynomial fit. In some instances, the observations suffered from poor seeing and intermittent clouds, and we had to increase the exposure time. Our observational log is listed in Table 2, which includes the names of objects we observed, the observational time, the Heliocentric Julian Date (HJD), exposure time and the signal to noise (S/N) values. On each night, we also observed at least one of several rapidly rotating early-type stars: HR 7894 (B5 IV, $v \sin i = 330\ \mathrm{km\ s^{-1}}$); HR 1051 (B8 V, $v \sin i = 334\ \mathrm{km\ s^{-1}}$); HR 8858 (B5 V, $v \sin i = 332\ \mathrm{km\ s^{-1}}$) and HR 989 (B5 V, $v \sin i = 298\ \mathrm{km\ s^{-1}}$) as telluric templates. If the telluric lines in the spectra of our objects were heavy, we removed their telluric lines using these telluric templates obtained by the telluric subpackage that is part of IRAF. A detailed description of the method and an example of this procedure was provided by Gu et al. (2002).

Table 2 The Observational Log of Objects in Our Study

Name	Date	HJD	Exp. time	S/N					
		2 400 000+	(s)	Na I	Hα	Li λ6708	Ca II IRTλ8498	Ca II IRTλ8542	Ca II IRTλ8662
V368 Cep	2009/12/30	55196.6672	6600	87	117	122	106	117	109
V368 Cep	2009/12/31	55197.7564	6014	70	93	96	87	96	91
V368 Cep	2010/02/03	55231.5982	3600	105	142	144	123	137	127
V368 Cep	2010/02/03	55231.6837	3600	94	129	131	113	124	116
V368 Cep	2010/02/04	55232.6867	4800	118	157	162	136	153	143
DX Leo	2009/12/29	55195.9541	7200	78	97	100	82	93	86
DX Leo	2009/12/30	55196.8813	4200	67	85	87	75	84	77
DX Leo	2009/12/31	55197.8785	3600	85	111	113	97	110	101
DX Leo	2010/01/04	55201.8541	10800	74	93	95	82	90	84
DX Leo	2010/02/02	55230.7520	3600	83	105	107	90	101	95
DX Leo	2010/02/03	55231.8929	2400	92	119	120	98	111	104
DX Leo	2010/02/04	55232.9866	7200	92	123	128	114	126	117
EP Eri	2009/12/30	55196.7344	2400	65	89	90	82	91	84
EP Eri	2009/12/31	55197.8114	2400	48	71	75	73	82	76
EP Eri	2010/01/04	55201.6669	5400	66	87	89	77	86	79
EP Eri	2010/02/02	55230.6406	3600	88	130	134	121	138	128
EP Eri	2010/02/03	55231.6520	2400	117	169	176	160	178	166
EP Eri	2010/02/04	55232.6437	1800	103	153	160	146	162	150
GJ 211	2009/12/29	55195.9007	1800	51	65	65	55	62	56
GJ 211	2009/12/30	55196.8169	1800	84	107	109	92	101	92
GJ 211	2009/12/31	55197.8544	1800	97	115	118	99	112	102
GJ 211	2010/01/04	55201.7513	5400	90	117	118	99	110	102
GJ 211	2010/02/02	55230.6949	3000	105	126	128	99	113	104
GJ 211	2010/02/03	55231.7340	1500	321	449	453	413	455	420
GJ 211	2010/02/04	55232.7410	1200	101	127	129	107	117	107
PW Aad	2008/09/20	54730.7870	3600	83	108	112	100	108	103
PW And	2009/12/01	55167.6288	7200	80	104	110	96	107	99
PW And	2010/01/02	55199.6644	7200	49	69	69	65	71	66
V383 Lac	2009/12/01	54729.7298	3600	60	79	80	70	76	71
V383 Lac	2010/01/02	54730.7425	3600	43	55	57	50	55	52

3 SPECTROSCOPIC ANALYSIS AND DIAGNOSTIC TECHNIQUE

We briefly discuss the Li 6708 line, chromospheric activity indicators and the diagnostic technique we used in this analysis.

3.1 The Li I Line

The Li I 6708 Å line is an important indicator of age because it is destroyed by thermonuclear reactions in stellar interiors.

3.2 Chromospheric Activity Indicators

Chromospheric activity produces a filling-in or emission in some strong photospheric lines. Typically, we use the strong lines as chromospheric activity indicators (Montes et al. 2004; Zhang 2011). These indicators are summarized as follows:

The Na I D_1 and D_2 lines

The Na I D_1 (5896 Å) and D_2 (5890 Å) lines are formed in the upper photosphere and lower chromosphere. They are detected as an emission reversal during flares or as filled-in absorption

(Andretta et al. 1997; Montes et al. 1997; Montes et al. 2004).

The Ca II IRT lines

The Ca II IRT lines (8498 Å, 8542 Å and 8662 Å) are very important optical chromospheric activity indicators (Gunn & Doyle 1997; Montes et al. 1997; Montes et al. 2000). They are formed in the lower chromosphere. The ratio of excess emission, EW_{8542}/EW_{8498}, is also an indicator of the chromospheric structure of plages and prominences. The value of EW_{8542}/EW_{8498} is around 1–3 for solar and stellar plages (Chester 1991; Lazaro & Arevalo 1997; Montes et al. 1997), but the value is above 3 for prominences (Chester 1991).

The Hα, Hβ and other Balmer lines

The Balmer lines (Hα (6563 Å), Hβ (4861 Å), H_γ (4341 Å), etc) are very useful indicators of chromospheric activity and are formed in the middle chromosphere. For less active stars, their profiles show filled-in absorption. However, their emissions are above the continuum for many active stars. Furthermore, the ratio of $EW_{H\alpha}/EW_{H\beta}$ can also be used as a diagnostic indicator for discriminating between plages and prominences (Hall & Ramsey 1992; Montes et al. 2004), and as a diagnostic tool for the presence of non-thermal electrons (Kashapova et al. 2008). According to the Buzasi model (Buzasi 1989), a low ratio (1–2) indicates the presence of a plage or prominence viewed against the stellar disk, but a high ratio (> 3, to a theoretical maximum of about 15) signals extended regions viewed off the limb of the star (Hall & Ramsey 1992).

The Ca II H & K lines

The Ca II H (3968 Å) & K (3933 Å) lines have been traditional chromospheric indicators (Montes et al. 2004; Zhao et al. 2013). They are formed in the middle chromosphere, and the corresponding core emissions signify normal behavior in chromospheric activity.

The He I lines

The He I D_3 5876 Å and He I 10830 Å lines are formed in the upper chromosphere (Shcherbakov et al. 1996; Houdebine et al. 2009). Emission of these lines above the continuum indicates the presence of a flare event (Zirin 1988; Montes et al. 1999).

Our observational spectral region is about 5600–9100 Å, which includes the Na I D_1 and D_2 lines, the Hα line, the Ca II IRT lines and the He I D_3 line. We can use these indicators to investigate chromospheric activities.

3.3 The Spectral Analysis Technique

To decern the contribution from chromospheric activity, the spectral subtraction technique is commonly employed. The principle behind this method is that chromospheric contribution equals the observed spectra minus the synthesized spectra. The key aspect of this technique is to construct a reasonable synthesized spectrum representing the underlying contribution from the photosphere. There are two methods that are utilized. One is to use theoretical spectra based on the radiation transfer equation (Fraquelli 1984), while the other employs the observed spectra of inactive stars (Barden 1985; Herbig 1985; Eker et al. 1995; Gunn & Doyle 1997; Frasca et al. 2000b; etc).

The normalized spectra from our samples were analyzed using the second method and by using the STARMOD program (Barden 1985; Montes et al. 1995, 2000; etc). During the analysis, the template and $v \sin i$ values of our objects were determined using spectra with wavelength ranges of 6389–6477 Å and 6615–6706 Å (Zhang & Gu 2008). An example of the subtracted (the observed spectra minus the synthesized one), observed and synthesized spectra in the wavelength range 6395–6435 Å based on three different template stars is displayed in Figure 1.

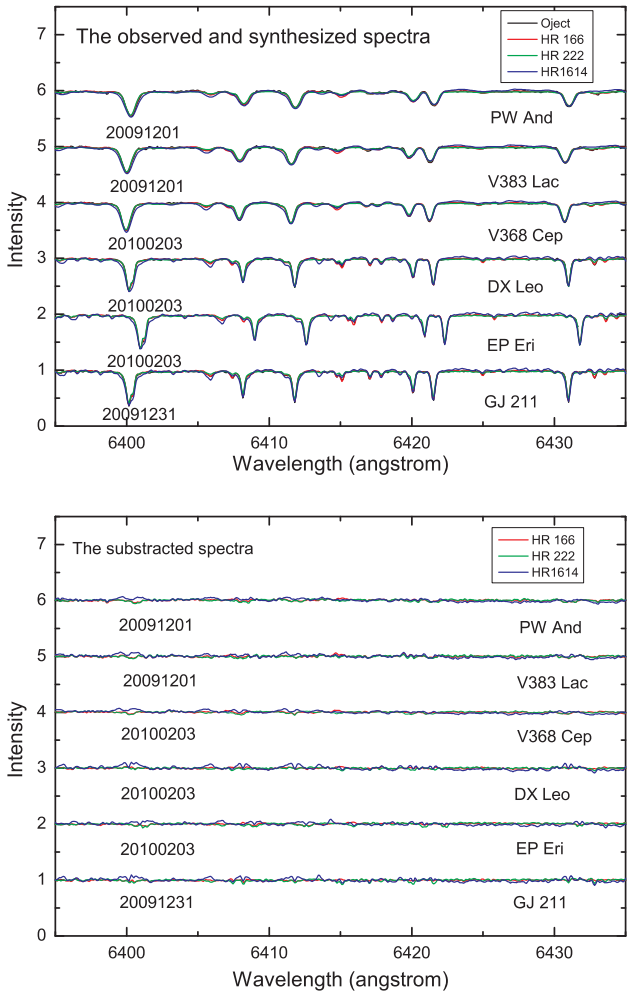

Fig. 1 Samples of the observed, synthesized and subtracted spectra in 6395–6435 Å derived by the different inactive samples. The number below each spectrum in this figure represents the observation date (year month day). The same rule applies in Fig. 2–8.

For all our objects, the templates of HR 166 (K0 V) and HR 222 (K2.5 V) are better than the other templates, such as HR 1614 (K3 V) (see Fig. 1). For V368 Cep, EP Eri and GJ 211, the template of HR 166 is better than that of HR 222 and HR 1614, but for DX Leo, PW And and V383 Lac, the template of HR 166 is similar to HR 222. Because the signal to noise of HR 166 is higher than that of HR 222, we therefore choose HR 166 as the template. These values (V368 Cep: 15 km s^{-1}; DX Leo: 6.8 km s^{-1}; EP Eri: 3 km s^{-1}; GJ 211: 3 km s^{-1}; PW And: 21.6 km s^{-1}; and V383 Lac: 19.4 km s^{-1}) were close to the results derived by Montes et al. (2001a). We fixed our results of $v \sin i$ to analyze all the spectra. Samples of the subtracted, observed and synthesized spectra with the He I D_3, Na I D_1, D_2, Hα and Ca II IRT 8542 lines are plotted in Figure 2. Moreover, all these spectra of the different objects are displayed in Figures 3–8.

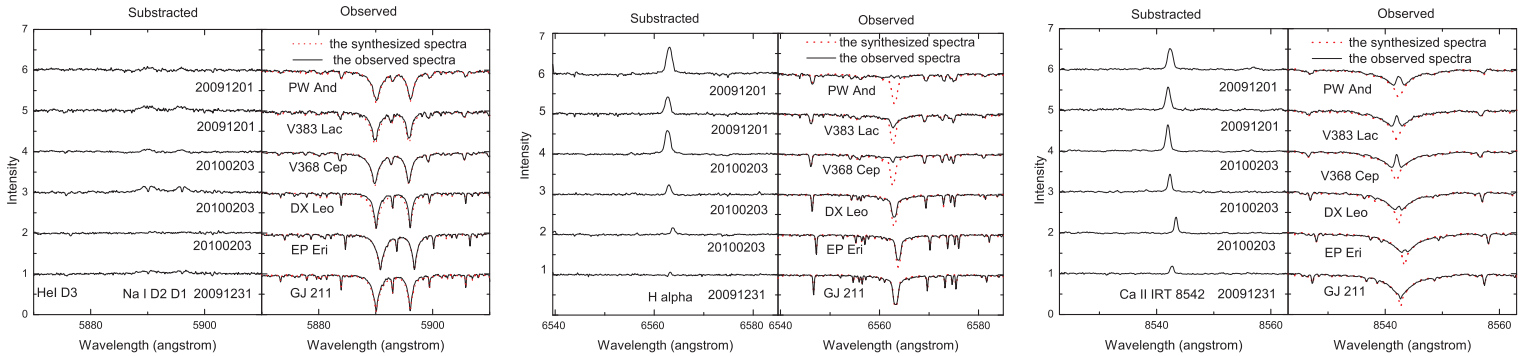

Fig. 2 Samples of the observed, synthesized and subtracted spectra of our objects with the He I D_3, Na I D_1, D_2, Hα and Ca II IRT 8542 lines.

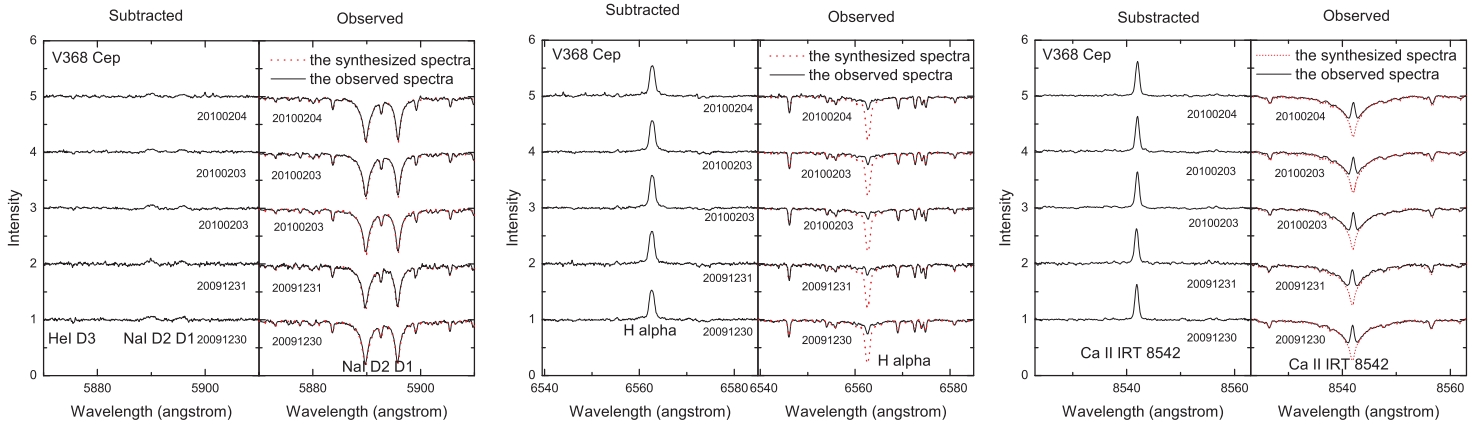

Fig. 3 All the observed, synthesized and subtracted spectra of V368 Cep in the He I D_3, Na I D_1, D_2, Hα and Ca II IRT 8542 lines.

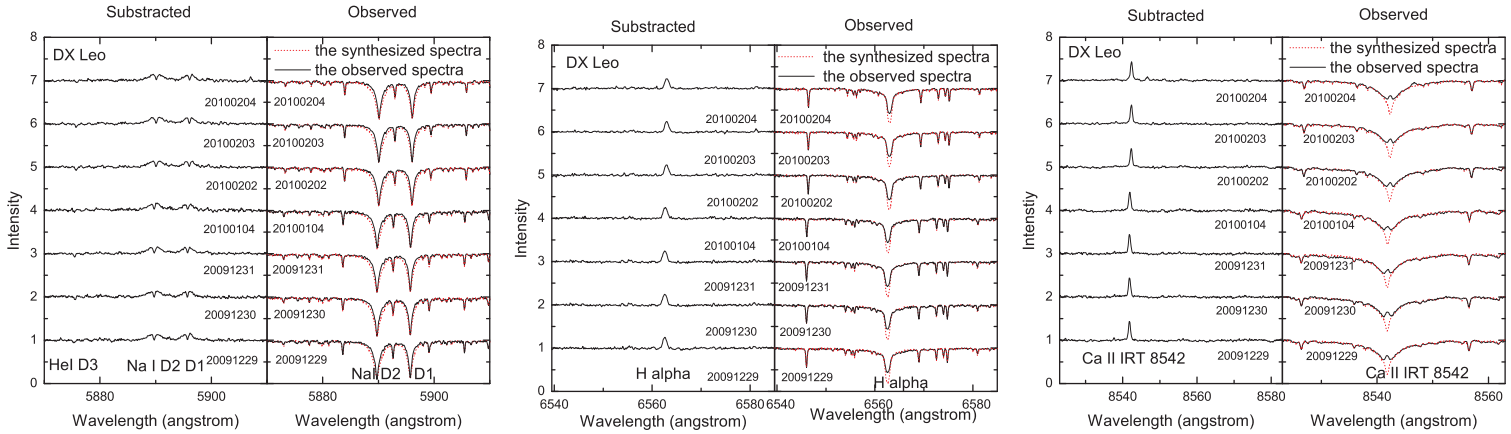

Fig. 4 The same spectra for DX Leo.

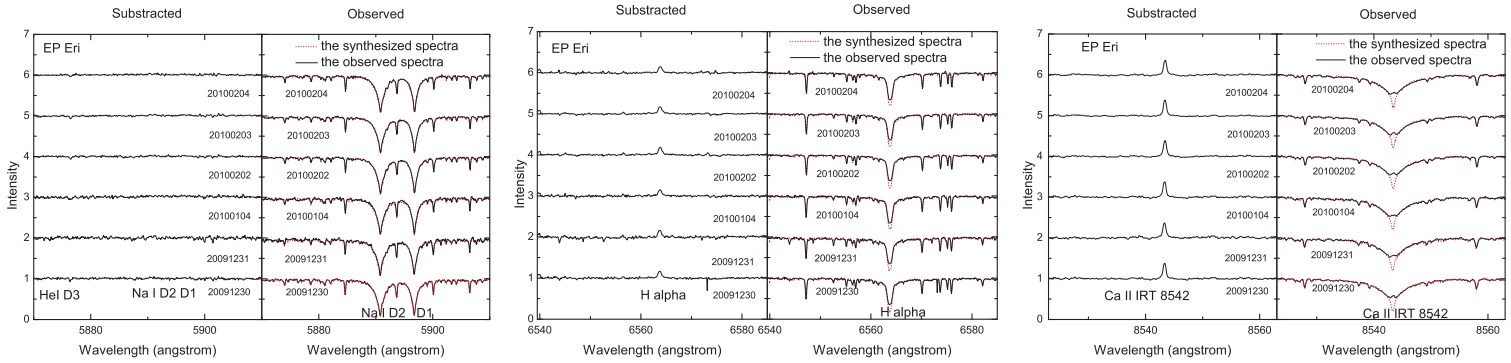

Fig. 5 The same spectra for EP Eri.

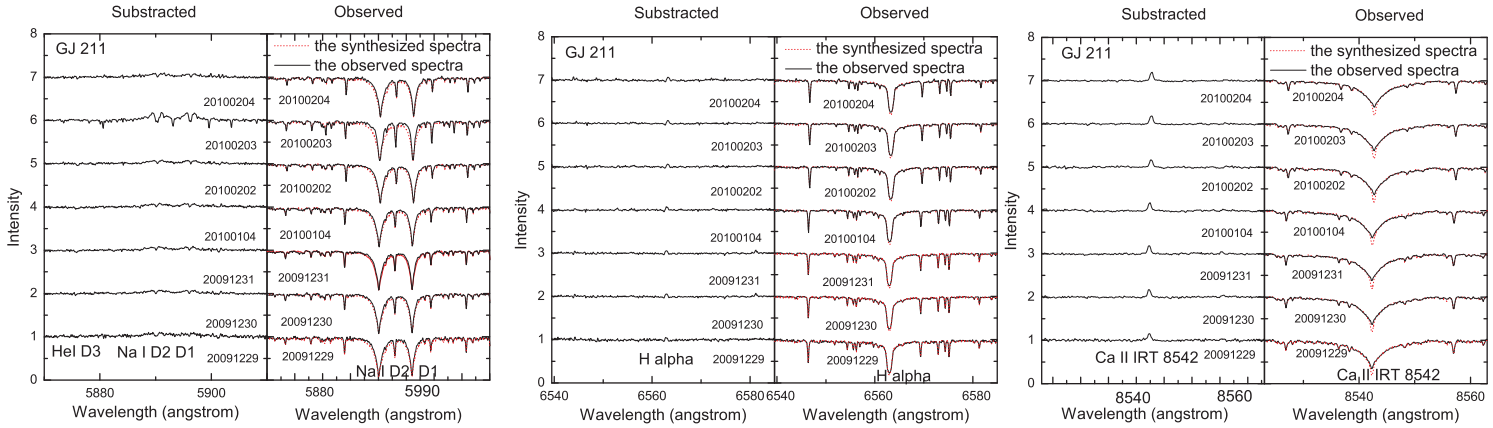

Fig. 6 The same spectra for GJ 211.

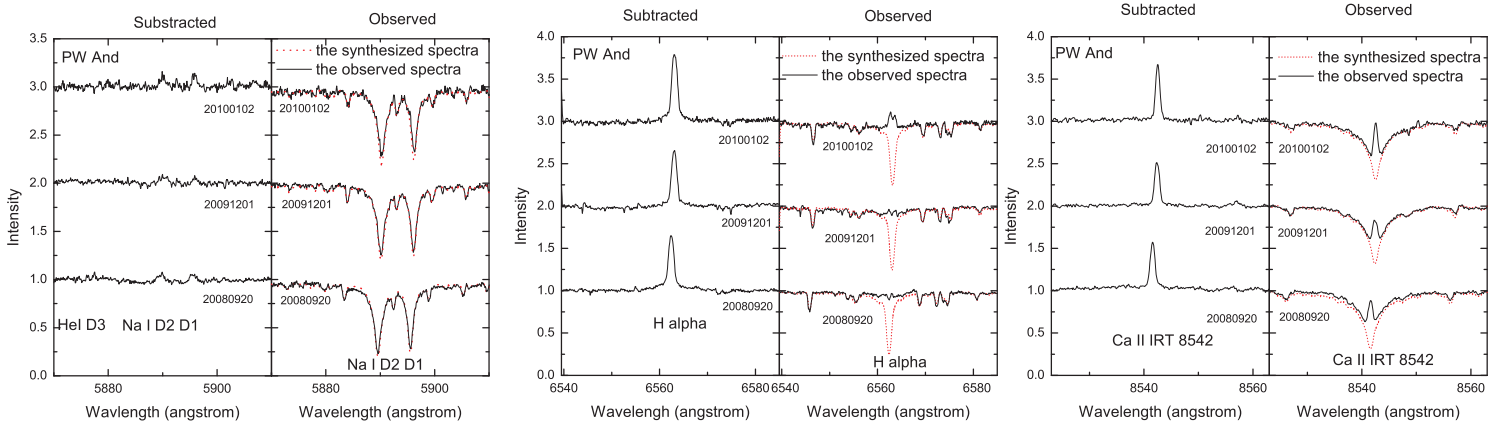

Fig. 7 The same spectra for PW And.

The equivalent widths (EWs) of the excess emissions were measured on the subtracted spectra by integrating over the emission profile with the IRAF SPLOT package. The details of the method were described in our previous paper (Zhang & Gu 2008). We listed the EWs of the chromospheric emissions in Table 3. Because the Li I line is blended with the nearby Fe I 6707.41 Å (when $v \sin i > 8\ \mathrm{km\ s^{-1}}$), the equivalent width of the Li I was calculated by subtracting the EW of the Fe I 6707.41 line (Montes et al. 2001a), which could be obtained from the relationship derived by Soderblom et al. (1993a). The phases were calculated using the equation at the bottom of Tables 3 and 4.

4 INDIVIDUAL RESULTS

We describe the individual results related to chromospheric activity shown by our objects in the following.

4.1 V368 Cep

V368 Cep (K1 V, $v \sin i = 16.1\ \mathrm{km\ s^{-1}}$, $P_{\mathrm{orb}} = 2.75^{\mathrm{d}}$) is the optical counterpart of X-ray source H2311+77 (Fekel 1997; Nugent et al. 1983; Pravdo et al. 1985; Kahanpää et al. 1999). Observations of this target have observed a starspot (Poretti et al. 1985; Bianchi et al. 1991; Mantegazza et al. 1992; Kahanpää et al. 1999), chromospheric emission (Joy & Wilson 1949; Montes et al. 2001a), transition region emission (Bianchi et al. 1991); coronal X-ray events (Pravdo et al. 1985; Pandey & Singh 2008) and flare events (Bowyer et al. 1994; Pye et al. 1995).

The chromospheric activity in V368 Cep was first detected as strong emission in the Ca II H & K lines by Joy & Wilson (1949). Later, Montes et al. (2001a) observed strong and variable excess chromospheric emissions in the Balmer lines, and the Ca II IRT in the emission was superimposed on the corresponding absorption. Our five spectra confirm the behavior of chromospheric activities (Figs. 2 and 3). To compare our results with published data, we collected all published EWs in Table 4. All the EWs in the Hα and Ca II IRT lines are plotted vs. the orbital phase in Figure 9 and vs. HJD in Figure 10. As can be seen from these figures, all our results on chromospheric activity indicators confirmed the previous results. However, the data in the present paper are not enough to study the modulations of V368 Cep, not only due to the sparse data sampling, but also the longer cadence of the new observations.

There were two Li observations with EWs of 288 mÅ (Poretti et al. 1985) and 207 mÅ (Montes et al. 2001a). Our result was 249 ± 4 mÅ, which is slightly larger than the result of Montes et al. (2001a) but smaller than that of Poretti et al. (1985). This might be caused by the normalization and possible blending of the spectral lines, or other reasons. These values confirm that V368 Cep is a possible member of the Local Association moving group (Poretti et al. 1985; Montes et al. 2001a,b; Martínez-Arnáiz et al. 2011), the age of which is about 20 to 150 Myr (Montes et al. 2001a,b; etc).

4.2 DX Leo

DX Leo (K0 V, $v \sin i = 6.2\ \mathrm{km\ s^{-1}}$, P_{orb} = 5.38^{d}) is a nearby young active star (Fekel 1997). Observations of this target have observed a starspot (Henry et al. 1995a; Messina & Guinan 1996; Strassmeier et al. 1997; Messina et al. 1999), chromospheric emission (Baliunas et al. 1995, 1996; Montes et al. 2001a), transition region emission (Soderblom & Clements 1987), and coronal X-ray and EUV events (Pye et al. 1995; Hünsch et al. 1999).

DX Leo shows noticeable excess emission in the Ca II H & K (Basri et al. 1989), Ca II IRT and Hα lines (Montes et al. 2001a). For our seven spectra from DX Leo (see Fig. 4), the Ca II IRT lines show strong filled-in absorption with a weak emission core, and the subtracted spectra show clear emission. All our results are similar to the previous results (Figs. 9 and 10). The Hα line shows weak filled-in absorption. Moreover, the subtracted profile shows excess emission. Our value for EW (Li)

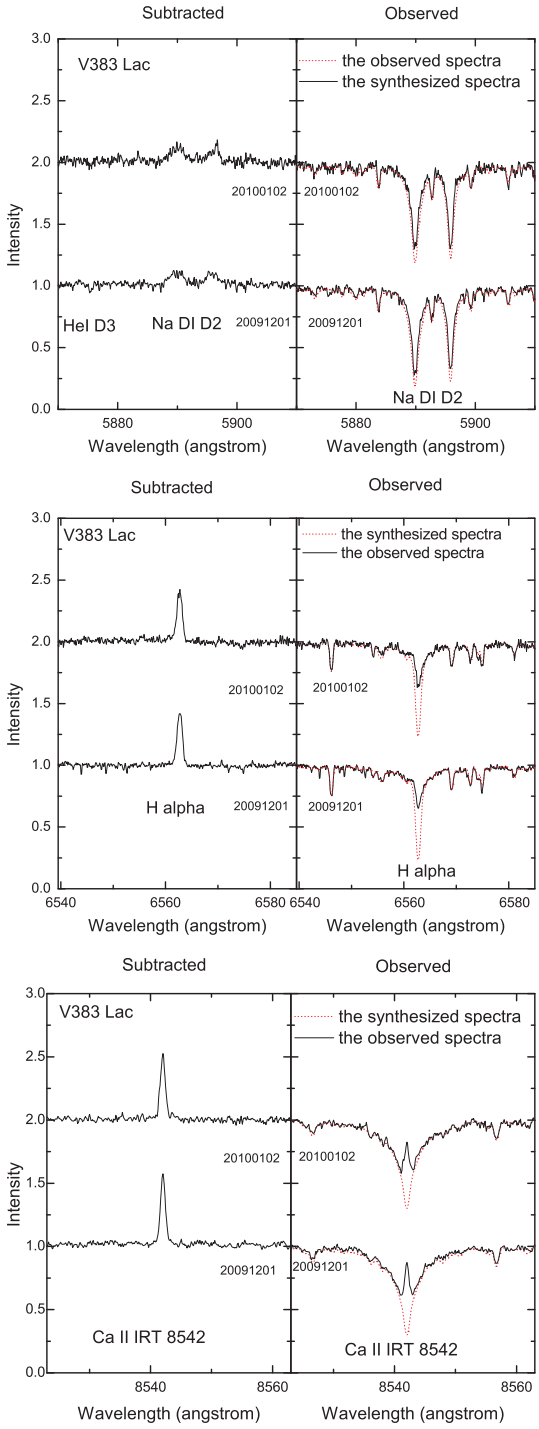

Fig. 8 The same spectra for V383 Lac.

Table 3 EWs of excess chromospheric emissions from our objects in the Na I D_1, D_2, Hα and Ca II IRT lines.

Name	HJD (2400000+)	Phase	$EW_{Na_I D_1}$ (Å)	$EW_{Na_I D_2}$ (Å)	$EW_{H\alpha}$ (Å)	$EW_{Ca_{II}\ 8498}$ (Å)	$EW_{Ca_{II}\ 8542}$ (Å)	$EW_{Ca_{II}\ 8662}$ (Å)	EW_{8542}/EW_{8498}	$EW_{Li\ I}$ (Å)
PW And	54730.7870	0.450	0.143±0.002	0.126±0.001	1.220±0.01	0.552±0.008	0.639±0.022	0.518±0.007	1.158 ± 0.019	0.286±0.002
PW And	55167.6288	0.074	0.116±0.020	0.056±0.001	1.041±0.03	0.505±0.020	0.597±0.006	0.514±0.003	1.182 ± 0.035	0.278±0.004
PW And	55199.6644	0.380	0.143±0.005	0.130±0.003	1.365±0.01	0.561±0.020	0.640±0.006	0.587±0.015	1.141 ± 0.030	0.277±0.003
V383 Lac	54729.7298	0.554	0.257±0.017	0.197±0.010	0.549±0.001	0.484±0.016	0.657±0.010	0.512±0.015	1.357±0.024	0.272 ±0.002
V383 Lac	54730.7425	0.972	0.336±0.012	0.230±0.035	0.547±0.007	0.439±0.022	0.646±0.009	0.511±0.027	1.469±0.053	0.270 ±0.014
V368 Cep	55196.6672	0.908	0.115±0.008	0.074±0.009	0.923±0.025	0.499±0.034	0.591±0.002	0.515±0.011	1.184 ±0.077	0.226 ±0.005
V368 Cep	55197.7564	0.305	0.103±0.004	0.070±0.001	0.999±0.001	0.528±0.045	0.699±0.021	0.576±0.008	1.324 ±0.073	0.228 ±0.003
V368 Cep	55231.5982	0.656	0.119±0.009	0.066±0.005	0.969±0.020	0.515±0.005	0.638±0.003	0.563±0.014	1.239 ±0.006	0.224 ±0.005
V368 Cep	55231.6837	0.687	0.114±0.010	0.077±0.007	0.984±0.017	0.507±0.020	0.651±0.007	0.564±0.025	1.284 ±0.037	0.224 ±0.002
V368 Cep	55232.6867	0.054	0.096±0.001	0.060±0.004	0.992±0.014	0.518±0.012	0.651±0.007	0.590±0.037	1.257 ±0.016	0.222 ±0.001
DX Leo	55195.9541	0.489	0.431±0.022	0.347±0.003	0.240±0.004	0.254±0.011	0.377±0.012	0.322±0.002	1.484±0.017	0.184±0.007
DX Leo	55196.8813	0.662	0.360±0.020	0.229±0.010	0.299±0.016	0.279±0.009	0.398±0.013	0.368±0.030	1.427±0.001	0.204±0.007
DX Leo	55197.8785	0.847	0.359±0.051	0.293±0.307	0.298±0.003	0.253±0.010	0.358±0.019	0.335±0.019	1.415±0.019	0.184±0.009
DX Leo	55201.8541	0.587	0.385±0.015	0.241±0.027	0.274±0.001	0.265±0.001	0.351±0.026	0.369±0.020	1.325±0.093	0.198±0.011
DX Leo	55230.7520	0.961	0.399±0.020	0.235±0.030	0.252±0.003	0.270±0.026	0.386±0.020	0.341±0.023	1.430±0.064	0.180±0.003
DX Leo	55231.8929	0.173	0.501±0.040	0.310±0.033	0.244±0.002	0.277±0.002	0.395±0.022	0.382±0.030	1.426±0.069	0.179±0.001
DX Leo	55232.9866	0.377	0.459±0.024	0.268±0.033	0.250±0.001	0.270±0.017	0.406±0.046	0.345±0.014	1.493±0.076	0.187±0.005
EP Eri	55196.7344	0.173			0.170±0.014	0.227±0.017	0.293±0.006	0.264±0.006	1.291±0.070	0.206±0.011
EP Eri	55197.8114	0.330			0.161±0.001	0.231±0.005	0.316±0.026	0.241±0.011	1.368±0.083	0.201±0.005
EP Eri	55201.6669	0.893			0.162±0.010	0.200±0.006	0.295±0.005	0.232±0.012	1.475±0.019	0.203±0.005
EP Eri	55230.6406	0.123			0.185±0.012	0.220±0.005	0.309±0.001	0.261±0.016	1.405±0.033	0.214±0.004
EP Eri	55231.6520	0.270			0.192±0.002	0.237±0.014	0.309±0.026	0.267±0.001	1.304±0.131	0.204±0.012
EP Eri	55232.6437	0.415			0.166±0.022	0.200±0.005	0.330±0.034	0.249±0.017	1.550±0.241	0.200±0.012
GJ 211	55195.9007	0.374			0.021±0.001	0.111±0.002	0.133±0.013	0.124±0.002	1.198±0.096	0.025±0.001
GJ 211	55196.8169	0.458			0.027±0.004	0.101±0.002	0.129±0.004	0.129±0.006	1.277±0.014	0.020±0.001
GJ 211	55197.8544	0.554			0.028±0.001	0.110±0.001	0.149±0.011	0.125±0.007	1.355±0.100	0.028±0.001
GJ 211	55201.7513	0.913			0.034±0.002	0.130±0.015	0.151±0.011	0.161±0.002	1.162±0.049	0.017±0.002
GJ 211	55230.6949	0.578			0.037±0.003	0.133±0.002	0.140±0.008	0.149±0.001	1.053±0.044	0.035±0.005
GJ 211	55231.7340	0.674			0.032±0.005	0.147±0.010	0.152±0.003	0.169±0.009	1.034±0.050	0.015±0.001
GJ 211	55232.7410	0.766			0.032±0.001	0.145±0.009	0.151±0.003	0.167±0.002	1.041±0.044	0.017±0.002

Notes: The phases of PW And, V383 Lac, V368 Cep, DX Leo, EP Eri and GJ 211 were calculated using the formula Min.I = JD(Hel.) $2449284.0 + 1.75^{d}E$, Min.I = JD(Hel.) $2453961.25 + 2.42^{d}E$, Min.I = JD(Hel.) $2449284 + 2.74^{d}E$, Min.I = JD(Hel.) $2449284 + 5.377^{d}E$, Min.I = JD(Hel.) $2449284 + 6.85^{d}E$ and Min.I = JD(Hel.) $2449284 + 10.86^{d}E$.

of 188 ± 6 mÅ is similar to the value of 187 mÅ (Strassmeier et al. 2000), which is in the range shown by the Pleiades (Montes et al. 2001a; López-Santiago et al. 2006; Martínez-Arnáiz et al. 2011).

4.3 EP Eri

EP Eri is a young active star (Cutispoto 1992; Henry et al. 1995b). It has exhibited a starspot (Henry et al. 1995b) and chromospheric activity (Pasquini et al. 1988; Cayrel de Strobel & Cayrel 1989; Henry et al. 1995b; Montes et al. 2001a; etc). Its chromospheric activity has shown Ca II H & K emissions (Joy & Wilson 1949) and filled-in absorption in the Hα line (Pasquini et al. 1988; Henry et al. 1995a), and excess emissions of Ca II IRT lines (Montes et al. 2001a). For our six spectra in Figure 5, the behavior of the chromospheric indicators is close to the previous results (Figs. 9 and 10). Because most of the data show a large dispersion and there is a large gap in the data of EP Eri (Fig. 9), more data are needed to address the issue of rotation modulation. The EWs in the strong lithium line of EP Eri are 197 mÅ (Favata et al. 1995), 187 mÅ (Strassmeier et al. 2000) and 205 mÅ (Montes et al. 2001a). Our result is 205 ± 8 mÅ, which is similar to the previous results (Favata et al.

1995; Strassmeier et al. 2000). These values confirm that EP Eri is a possible member of the Local Association moving group (Pleiades) (Montes et al. 2001a,b; López-Santiago et al. 2006).

4.4 PW And

PW And is a fast rotating single star (Fekel 1997; Montes et al. 2001a,b; López-Santiago et al. 2010). It is characterized by photospheric activity, which is apparent from the light curve variation (Hooten & Hall 1990) and Doppler imaging (Strassmeier & Rice 2006; Gu et al. 2010), chromospheric activity (Bidelman 1985; Strassmeier et al. 1993; Christian et al. 2001; Montes et al. 2001a), transition region (Christian et al. 2001; Wood et al. 2000), several flare events (López-Santiago et al. 2003) and X-ray emission (Eker et al. 2008).

PW And shows moderate emissions of Ca II H & K (Bidelman 1985) and Hα lines (Christian et al. 2001; Montes et al. 2001a; López-Santiago et al. 2003). For our observed spectra (Figs. 2 and 7), the Na I D lines are characterized by deep absorption. The spectra computed after subtraction demonstrate that the cores of the Na I D_1 and D_2 lines exhibit weak excess emission. All the Ca II IRT lines display obvious self-reversal in the core. These spectra also reveal that the Ca II IRT lines show clear excess emissions. Our Hα line, taken on 2010 January 2, exhibits emission above the continuum (see Fig. 7). The subtracted spectra from PW And show strong excess emission of the Hα line. All our results are similar to the previous results (Figs. 9 and 10). There were several measurements of the lithium 6707.8 line, with EW values of 271 mÅ derived by Montes et al. (2001a), 298 mÅ (Wichmann et al. 2003), 267 mÅ (López-Santiago et al. 2003), 278 ± 4 mÅ (Strassmeier & Rice 2006) and 278 ± 4 mÅ (López-Santiago et al. 2010). For our spectra, the mean value of EW (Li) is 280 ± 3 mÅ, which is similar to the previous results. These values confirm that PW And is a possible member of the Local Association moving group (Montes et al. 2001a,b; López-Santiago et al. 2006; Martínez-Arnáiz et al. 2011).

4.5 V383 Lac

V383 Lac is a single active K1 V star (period = $2.42^{\rm d}$, $v \sin i = 15 \ {\rm km \ s^{-1}}$) within the Local Association moving group (Mulliss & Bopp 1994; Jeffries 1995; Henry et al. 1995b; Osten & Saar 1998; Biazzo et al. 2009). It presents typical magnetic active phenomena, which generate photospheric activity observable by light curve variation (Henry et al. 1995a; Robb et al. 1995; Xing et al. 2007b; Biazzo et al. 2009) or small radial velocity variation produced by a starspot (Biazzo et al. 2009), chromospheric activity (Mulliss & Bopp 1994; Biazzo et al. 2009) and coronal emission (Pounds et al. 1991; Pye et al. 1995).

V383 Lac is a very active chromospheric star, which shows emission cores in the Ca II H & K lines (Biazzo et al. 2009), filled-in absorption in the Hα and H_ϵ lines (Mulliss & Bopp 1994; Montes et al. 2001a); weak excess emissions in the Na I D_1 and D_2 lines; and filled-in absorption with core reversal of the Ca II IRT lines (Mulliss & Bopp 1994). There were four observations of Li 6708, with EW values of 250 mÅ obtained by Mulliss & Bopp (1994), 277 mÅ (Jeffries 1995), 257 mÅ obtained by Montes et al. (2001a) and 260 ± 10 mÅ (Biazzo et al. 2009). Our result is 271 ± 8 mÅ, which is similar to the previous results. These confirmed that V383 Lac is a star with a lithium abundance similar to the upper envelope of the Pleiades (Montes et al. 2001a,b; Martínez-Arnáiz et al. 2011; etc).

5 SUMMING UP

In this section, we will summarize the properties of the Li 6708 line, and the behavior of chromospheric activity. We believe that all our data are very important for any future discussions on the evolution of chromospheric activity.

5.1 The Li I 6708 Lines

We calculated the mean values of the lithium EWs for V368 Cep, EP Eri, DX Leo, GJ 211, PW And and V383 Lac. These confirmed that they are possible members of the Pleiades moving group (except for GJ 211) (Montes et al. 2001a,b; López-Santiago et al. 2006; Martínez-Arnáiz et al. 2011).

5.2 The Behavior of Chromospheric Activity

We obtained the level of chromospheric activity that resulted from our observing runs using several optical chromospheric activity indicators. For the Na I D1 and D2 lines, all our observed spectra show deep absorption. For the excess subtracted spectra, there is weak excess emission (PW And, V383 Lac, V368 Cep and DX Leo) or little emission (EP Eri and GJ 211). For the Hα line, PW And exhibits variation from absorption to weak emission and the subtracted Hα spectra show obvious emission. For other objects, they exhibit filled-in absorption (V383 Lac and V368 Cep) or deep absorption (EP Eri, DX Leo and GJ 211). The corresponding subtracted cases show obvious excess emission (V383 Lac and V368 Cep) or weak emission (EP Eri, DX Leo and GJ 211). For the Ca II IRT lines, all these objects show clear filled-in absorption with core-emission (PW And, V383 Lac, V368 Cep, DX Leo and EP Eri) or have unobservable emission (GJ 211). It is well known that the He I D_3 line is a probe of flare-like events (Zirin 1988). For the He I D_3 lines of our 30 spectra, we did not observe any emission, which means there were no strong flare-like episodes during our observing sessions. There are not enough data in the present paper to study rotational modulations in the chromospheric activity of our targets.

The ratio of excess emission, EW_{8542}/EW_{8498}, is an indicator of plages and prominences. The ratios of our objects are about 1.3 (Table 3). These small ratios support the previous results (Montes et al. 2001a; etc) and indicate that there are optically thick emissions in plage-like regions. These values were also detected in stars with chromospheric activity investigated by previous authors: Lazaro & Arevalo (1997); Montes et al. (2000); Gu et al. (2002); Gálvez et al. (2009); and Zhang & Gu (2008).

6 DISCUSSION

We will discuss the relationship between the equivalent widths of the Li I 6708 line and rotation, and the relations between chromospheric activity and stellar rotation as exhibited by the average values of excess chromospheric emission, the maximum amplitudes of chromospheric rotational modulation and the ratios of excess emissions indicated by EW_{Ca8542}/EW_{Ca8498}.

6.1 The Relationship between the Equivalent Width of Li I and Stellar Rotation

We collected more data on other single stars in the Pleiades (Table 5) and investigated whether there exists a relationship between the equivalent widths of Li I 6708 Å and $v \sin i$ velocity. As can be seen from Figure 11, the EWs of Li I 6708 Å decrease with decreasing $v \sin i$ velocity. We used a simple linear function to fit the trend shown by the data (Table 6).

The relation confirms the result that was found in previous results (Rebolo & Beckman 1988; Tschäpe & Rüdiger 2001; Xing et al. 2007a). A model for lithium depletion with age (Piau & Turck-Chièze 2002) and the relation between age and rotation evolution (Bouvier et al. 1997; Xing et al. 2007a; etc) indicate that younger objects rotate faster, and that they still retain lithium in their atmospheres.

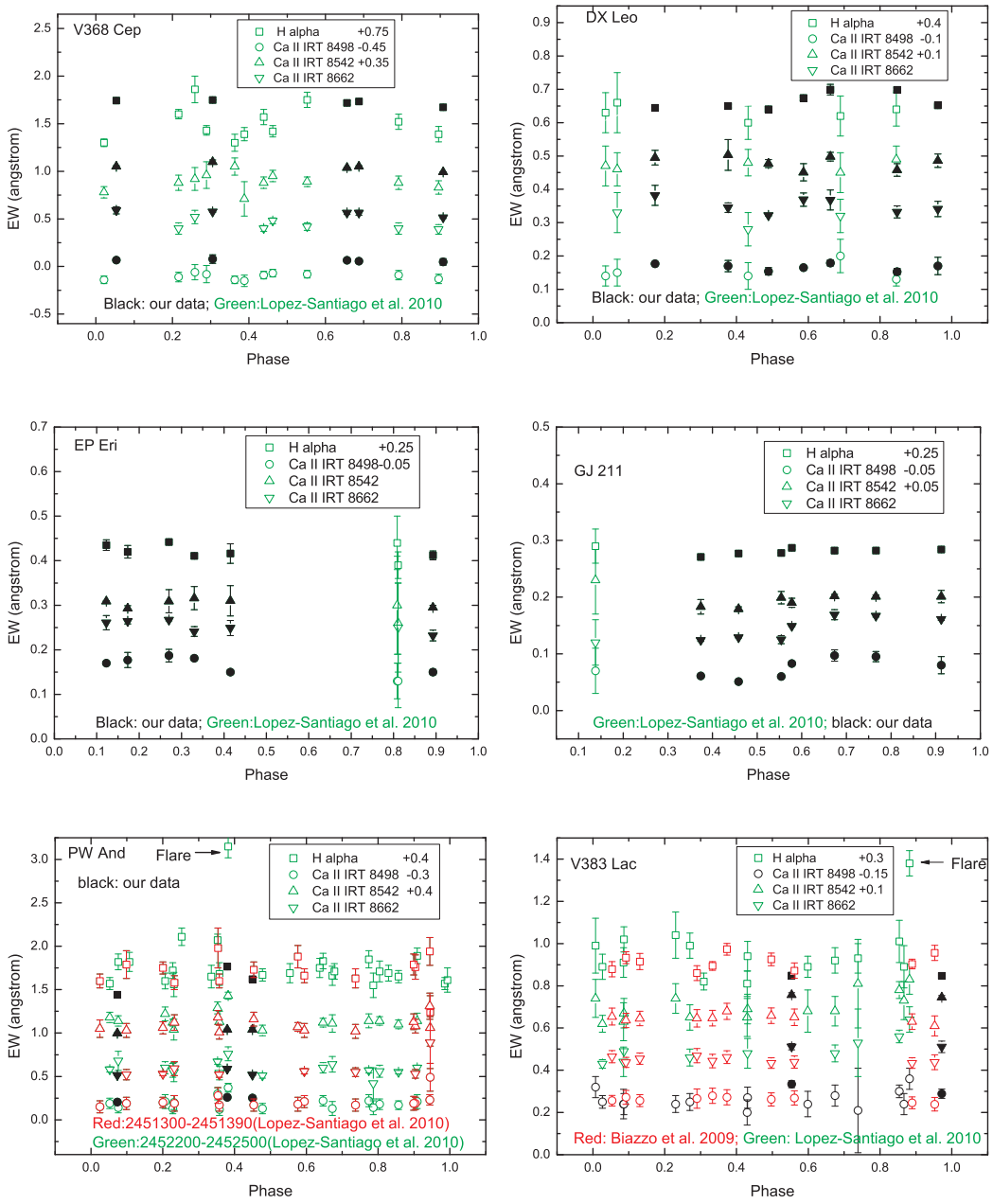

Fig. 9 All the chromospheric activity vs. the orbital phase for V368 Cep, EP Eri, DX Leo, GJ 211, PW And and V383 Lac in the Hα and Ca II IRT lines. The different/open colored points represent the data published by the different authors. The solid points represent our new data.

Table 4 All published data about excess emissions from our objects that are given in literature.

Name	HJD (2400000+)	Phase	$EW_{Na_I D_1}$ (Å)	$EW_{Na_I D_2}$ (Å)	$EW_{H\alpha}$ (Å)	$EW_{Ca_{II}\ 8498}$ (Å)	$EW_{Ca_{II}\ 8542}$ (Å)	$EW_{Ca_{II}\ 8662}$ (Å)	EW_{8542}/EW_{8498}	$EW_{Li\ I}$ (Å)	Ref.
PW AND	51384.1732	0.099			1.39±0.16	0.49±0.07	0.63±0.08	0.52±0.06	1.286 ± 0.020	0.2634±0.0017	[1]
PW AND	51385.0401	0.594			1.26±0.08	0.51±0.07	0.63±0.08	0.56±0.03	1.235 ± 0.013	0.2564±0.0017	[1]
PW AND	51386.1011	0.201			1.35±0.07	0.50±0.06	0.66±0.07	0.53±0.02	1.320 ± 0.018	0.2654±0.0017	[1]
PW AND	51387.0396	0.737			1.23±0.11	0.47±0.07	0.62±0.08	0.55±0.05	1.319 ± 0.026	0.2634±0.0017	[1]
PW AND	51388.1258	0.358			1.20±0.08	0.47±0.07	0.61±0.08	0.52±0.03	1.298 ± 0.023	0.2504±0.0017	[1]
PW AND	51389.0818	0.904			1.36±0.14	0.49±0.07	0.68±0.08	0.53±0.05	1.388 ± 0.035	0.2694±0.0017	[1]
PW AND	51508.8690	0.354			1.58±0.23	0.58±0.09	0.78±0.08	–	1.345 ± 0.070	0.2784±0.0017	[1]
PW AND	51509.9022	0.944			1.54±0.16	0.53±0.06	0.91±0.15	–	1.717 ± 0.089	0.2734±0.0017	[1]
PW AND	51767.6572	0.233			1.18±0.08	0.49±0.09	0.72±0.09	0.59±0.08	1.469 ± 0.086	0.2944±0.0017	[1]
PW AND	51770.6541	0.945			0.84±0.19	0.79±0.16	0.66±0.21	0.89±0.30	0.835 ± 0.097	0.3144±0.0017	[1]
PW AND	51854.5731	0.899			1.39±0.12	0.49±0.08	0.73±0.09	–	1.490 ± 0.059	0.2474±0.0017	[1]
PW AND	51855.5441	0.454			1.33±0.09	0.47±0.07	0.76±0.08	–	1.617 ± 0.071	0.2564±0.0017	[1]
PW AND	51856.5440	0.025			1.20±0.08	0.45±0.07	0.65±0.10	–	1.444 ± 0.002	0.2664±0.0017	[1]
PW AND	51857.5090	0.577			1.48±0.13	0.48±0.08	0.67±0.05	–	1.396 ± 0.128	0.2724±0.0017	[1]
PW AND	52176.4998	0.857			1.25±0.07	0.47±0.05	0.70±0.05	0.55±0.02	1.489 ± 0.052	0.2714±0.0017	[1]
PW AND	52177.5860	0.478			1.27±0.07	0.43±0.06	0.63±0.06	0.51±0.03	1.465 ± 0.065	0.2734±0.0017	[1]
PW AND	52263.6771	0.673			1.26±0.11	0.43±0.08	0.71±0.10	0.64±0.09	1.651 ± 0.075	0.2764±0.0017	[1]
PW AND	52264.6541	0.231			1.16±0.14	0.50±0.08	0.64±0.12	0.55±0.11	1.280 ± 0.035	0.2834±0.0017	[1]
PW AND	52265.6573	0.804			1.31±0.12	0.48±0.06	0.74±0.05	0.56±0.07	1.542 ± 0.089	0.2814±0.0017	[1]
PW AND	52266.6686	0.382	0.21±0.03	0.20±0.03	2.75±0.13	0.67±0.05	1.03±0.04	0.76±0.08	1.537 ± 0.055	0.2694±0.0017	[1]
PW AND	52269.6331	0.076			1.42±0.09	0.44±0.06	0.74±0.06	0.68±0.11	1.682 ± 0.093	0.2784±0.0017	[1]
PW AND	52270.6320	0.647			1.43±0.09	0.52±0.06	0.72±0.05	0.60±0.06	1.385 ± 0.064	0.2684±0.0017	[1]
PW AND	52271.6485	0.228			1.32±0.09	0.43±0.06	0.72±0.04	0.57±0.08	1.674 ± 0.141	0.2514±0.0017	[1]
PW AND	52272.6263	0.786			1.15±0.14	0.44±0.08	–	0.42±0.18	–	0.2644±0.0017	[1]
PW AND	52273.6263	0.358			1.28±0.13	0.42±0.07	0.73±0.12	0.54±0.08	1.738 ± 0.004	0.2584±0.0017	[1]
PW AND	52457.1121	0.207			1.20±0.09	0.51±0.08	0.82±0.08	0.60±0.07	1.608 ± 0.095	0.2474±0.0017	[1]
PW AND	52458.1048	0.774			1.45±0.10	0.52±0.07	0.74±0.08	0.57±0.03	1.423 ± 0.038	0.2714±0.0017	[1]
PW AND	52459.1177	0.353	0.13±0.05	0.11±0.05	1.67±0.07	0.60±0.07	0.89±0.07	0.67±0.03	1.483 ± 0.056	0.2584±0.0017	[1]
PW AND	52460.0909	0.909			1.49±0.09	0.51±0.08	0.74±0.09	0.60±0.03	1.451 ± 0.051	0.2614±0.0017	[1]
PW AND	52462.0915	0.052	0.11±0.03	0.08±0.02	1.17±0.07	0.49±0.06	0.78±0.06	0.58±0.03	1.592 ± 0.072	0.2584±0.0017	[1]
PW AND	52508.6869	0.678			1.31±0.09	–	–	–		–	[1]
PW AND	52509.6923	0.253			1.71±0.10	–	–	–		–	[1]
PW AND	52510.7007	0.829			1.29±0.09	–	–	–		–	[1]
PW AND	52511.5869	0.335			1.25±0.13	–	–	–		–	[1]
PW AND	52512.7255	0.986			1.17±0.07	–	–	–		–	[1]
PW AND	52512.7377	0.993			1.21±0.14	–	–	–		–	[1]
PW AND	52513.7195	0.554			1.29±0.11	–	–	–		–	[1]
PW AND	52514.6870	0.107			1.42±0.11	–	–	–		–	[1]
PW AND	52515.6157	0.638			1.35±0.11	–	–	–		–	[1]
V383 LAC	51384.0141	0.027	–	–	0.59±0.06	0.40±0.03	0.52±0.040	0.43±0.020	1.300±0.003	0.2478±0.0016	[2]
V383 LAC	51384.1565	0.085	–	–	0.61±0.07	0.39 ±0.070	0.53±0.090	0.44±0.070	1.359±0.013	0.2468±0.0016	[2]
V383 LAC	51384.9920	0.431	–	–	0.64±0.07	0.42±0.050	0.59±0.070	0.48±0.070	1.405±0.001	0.2548±0.0016	[2]
V383 LAC	51386.0848	0.882	–	–	1.08±0.06	0.51±0.050	0.73±0.070	0.64±0.060	1.431±0.003	0.2588±0.0016	[2]
V383 LAC	51387.0233	0.270	–	–	0.69±0.06	0.40± 0.040	0.55±0.060	0.46±0.040	1.375±0.013	0.2548±0.0016	[2]
V383 LAC	51388.0023	0.675	–	–	0.62±0.06	0.43±0.050	0.58 ±0.070	0.48±0.040	1.349±0.006	0.2588±0.0016	[2]
V383 LAC	51388.9987	0.086	–	–	0.72±0.04	0.39 ±0.050	0.57 ±0.070	0.49	1.462±0.008	0.2658±0.0016	[2]
V383 LAC	51767.0580	0.309	–	–	0.52±0.04	0.40 ± 0.07	0.53±0.06	0.43±0.06	1.325±0.082	0.2788±0.0016	[1]
V383 LAC	51768.0975	0.739	–	–	0.63±0.07	0.36 ± 0.20	0.71±0.21	0.53±0.16	1.972±0.512	0.2568±0.0016	[1]
V383 LAC	51853.9877	0.230	–	–	0.74±0.11	0.39 ± 0.04	0.64±0.07	–	1.641±0.011	0.2768±0.0016	[1]
V383 LAC	51854.8790	0.599	–	–	0.59±0.05	0.39 ± 0.06	0.58±0.10	–	1.487±0.028	0.2498±0.0016	[1]
V383 LAC	51855.8679	0.007	–	–	0.69±0.13	0.47 ± 0.05	0.64±0.09	–	1.362±0.047	0.2928±0.0016	[1]
V383 LAC	51856.8901	0.430	–	–	0.51±0.06	0.35 ± 0.06	0.55±0.09	–	1.571±0.012	0.2518±0.0016	[1]
V383 LAC	51857.9473	0.867	–	–	0.59±0.10	0.39 ± 0.05	0.63±0.09	0.56±0.03	1.615±0.024	0.2518±0.0016	[1]
V383 LAC	52174.9359	0.854	–	–	0.71±0.10	0.45 ± 0.03	0.68±0.04	0.50±0.06	1.511±0.012	0.2548±0.0016	[1]
V383 LAC	53961.379	0.053			0.579±0.036	0.406±0.025	0.554±0.040	0.464±0.029	1.365±0.015		[3]

Table 4 —*Continued*

Name	HJD (2400000+)	Phase	$EW_{Na\,I\,D_1}$ (Å)	$EW_{Na\,I\,D_2}$ (Å)	$EW_{H\alpha}$ (Å)	$EW_{Ca\,II\ 8498}$ (Å)	$EW_{Ca\,II\ 8542}$ (Å)	$EW_{Ca\,II\ 8662}$ (Å)	EW_{8542}/EW_{8498}	$EW_{Li\,I}$ (Å)	Ref.
V383 LAC	53961.473	0.092			0.633±0.028	0.422±0.033	0.536±0.034	0.437±0.024	1.270±0.019		[3]
V383 LAC	53961.566	0.131			0.615±0.038	0.406±0.028	0.545±0.034	0.455±0.027	1.342±0.009		[3]
V383 LAC	53962.453	0.497			0.625±0.030	0.412±0.031	0.558±0.037	0.434±0.025	1.354±0.012		[3]
V383 LAC	53962.609	0.562			0.572±0.036	0.419±0.034	0.551±0.039	0.439±0.029	1.315±0.014		[3]
V383 LAC	53963.402	0.889			0.603±0.023	0.396±0.028	0.530±0.037	0.434±0.025	1.338±0.001		[3]
V383 LAC	53963.555	0.952			0.656±0.036	0.389±0.032	0.510±0.047	0.438±0.035	1.311±0.013		[3]
V383 LAC	53964.371	0.290			0.560±0.035	0.416±0.046	0.546±0.041	0.469±0.034	1.313±0.047		[3]
V383 LAC	53964.477	0.333			0.594±0.021	0.429±0.036	0.547±0.037	0.444±0.032	1.275±0.021		[3]
V383 LAC	53964.574	0.374			0.673±0.028	0.422±0.036	0.579±0.038	0.462±0.030	1.372±0.027		[3]
V368 CEP	51384.0420	0.439	1.25	0.68	0.82±0.08	0.36±0.04	0.48±0.06	0.40±0.03	1.333 ±0.019	0.2083±0.0008	[2]
V368 CEP	51385.0085	0.791	–	0.65	0.77±0.08	0.36±0.05	0.48±0.07	0.40±0.06	1.333 ±0.009	0.2013±0.0008	[2]
V368 CEP	51386.1725	0.216	0.87	0.59	0.85±0.05	0.34±0.05	0.48±0.08	0.40±0.06	1.412 ±0.028	0.2103±0.0008	[2]
V368 CEP	51387.0935	0.552	0.97	0.61	1.00±0.08	0.37±0.04	0.49±0.05	0.42±0.04	1.324 ±0.008	0.2043±0.0008	[2]
V368 CEP	51388.0347	0.896	0.93	0.65	0.64±0.08	0.32±0.05	0.43±0.07	0.39±0.05	1.344 ±0.009	0.1883±0.0008	[2]
V368 CEP	51389.0296	0.259	1.23	0.78	1.11±0.14	0.39±0.08	0.52±0.12	0.52±0.07	1.333 ±0.034	0.2053±0.0008	[2]
V368 CEP	51509.8749	0.363	1.07	–	0.55±0.09	0.31±0.07	0.65±0.09	–	2.097 ±0.020	0.1993±0.0008	[2]
V368 CEP	51854.9124	0.289			0.68±0.05	0.37±0.09	0.56±0.14	–	1.514 ±0.010	0.2153±0.0008	[1]
V368 CEP	51856.9186	0.021			0.55±0.04	0.31±0.04	0.38±0.06	–	1.226 ±0.035	0.2063±0.0008	[1]
V368 CEP	51857.9228	0.388			0.64±0.07	0.30±0.06	0.31±0.18	–	1.033 ±0.393	0.2193±0.0008	[1]
V368 CEP	52175.9666	0.463			0.67±0.06	0.38±0.04	0.55±0.06	0.48±0.03	1.447 ±0.006	0.2013±0.0008	[1]
DX LEO	51509.2471	0.845			0.24±0.05	0.23±0.02	0.39±0.04	–	1.696±0.026	0.1837±0.001	[1]
DX LEO	51510.2689	0.036			0.23±0.06	0.24±0.03	0.37±0.06	–	1.542±0.057	0.1797±0.001	[1]
DX LEO	51562.1797	0.690			0.22±0.06	0.30±0.05	0.35±0.06	0.32±0.05	1.167±0.006	0.1717±0.001	[1]
DX LEO	51564.2121	0.068			0.26±0.09	0.25±0.04	0.36±0.05	0.33±0.06	1.440±0.030	0.1797±0.001	[1]
DX LEO	51566.1720	0.432			0.20±0.05	0.24±0.04	0.38±0.04	0.28±0.05	1.583±0.097	0.1667±0.001	[1]
EP ERI	51508.9395	0.811	–	–	0.19±0.06	0.18±0.04	0.30±0.11	–	1.667±0.241	0.2110±0.0006	[2]
EP ERI	51769.2545	0.811			0.14 ±0.03	0.18 ±0.06	0.26±0.09	0.25 ±0.1	1.444±0.019	0.2150±0.0006	[1]
GJ 211	51566.0980	0.138	–	–	0.04±0.03	0.12±0.04	0.18±0.06	0.12±0.04	1.500±0.050		[2]

Notes: "–" No emission is detected. The phases of PW And, V383 Lac, V368 Cep, DX Leo, EP Eri and GJ 211 were calculated using the formula Min.I = JD(Hel.) 2449284.0 + 1.75^{d}E, Min.I =JD(Hel.) 2453961.25 + 2.42^{d}E, Min.I = JD(Hel.) 2449284 + 2.74^{d}E, Min.I = JD(Hel.) 2449284 + 5.377^{d}E, Min.I = JD(Hel.) 2449284 + 6.85^{d}E and Min.I = JD(Hel.) 2449284 + 10.86^{d}E. References: [1] López-Santiago et al. (2010); [2]Montes et al. (2001a); [3] Biazzo et al. (2009).

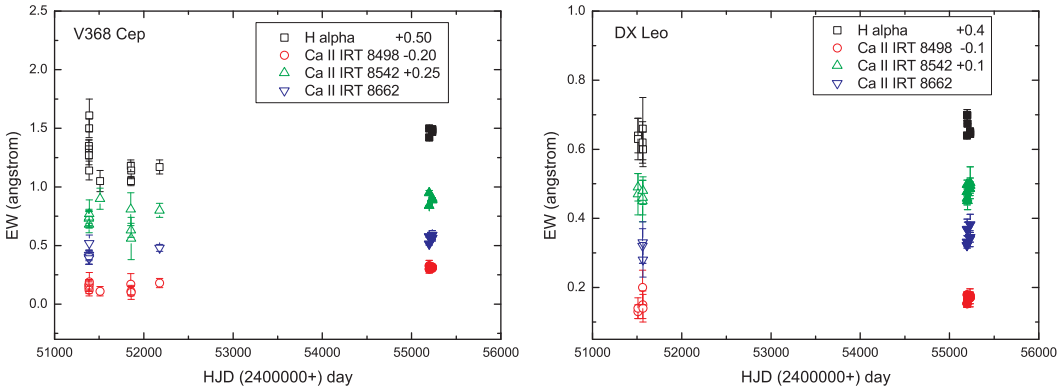

Fig. 10 The chromospheric activity vs. HJD for V368 Cep, EP Eri, DX Leo, GJ 211, PW And and V383 Lac in the Hα and Ca II IRT lines. The different open/colored points represent the previously published data on chromospheric activity indicators. The solid points represent our new data.

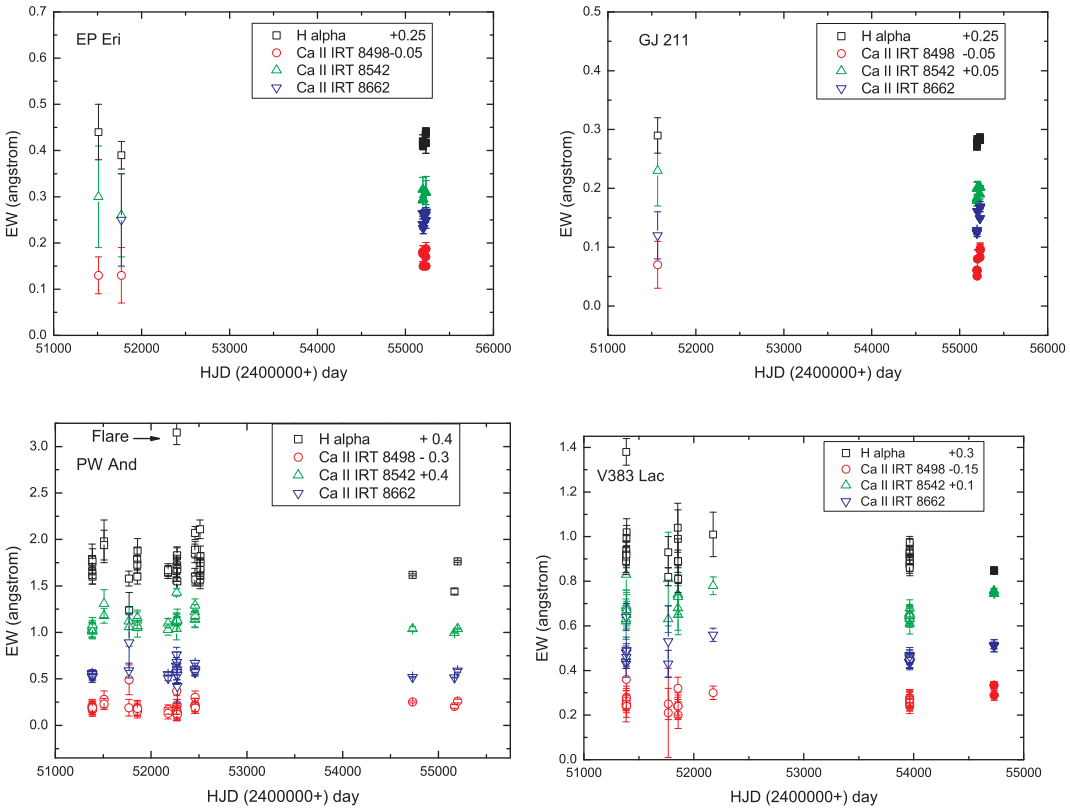

Fig. 10 — *Continued.*

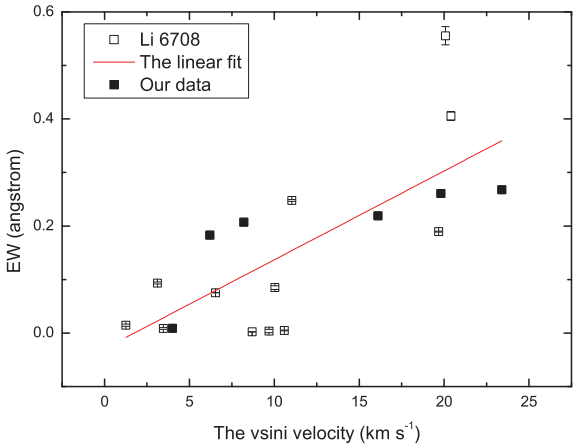

Fig. 11 The EWs of Li I 6708 vs. stellar $v \sin i$ velocity. The solid points represent our data and the open points represent the previously published data. The solid line shows a linear fit to all the available data.

Table 5 Average Values of the Excess Chromospheric Emissions from Objects in Our Study and Other Single Stars in the Pleiades

Name	Sp	$v \sin i$ (km s^{-1})	P (d)	EW$_{\rm Na\,I\,D_1}$ (Å)	EW$_{\rm Na\,I\,D_2}$ (Å)	EW$_{\rm H\beta}$ (Å)	EW$_{\rm H\alpha}$ (Å)	EW$_{\rm Ca\ 8498}$ (Å)	EW$_{\rm Ca\ 8542}$ (Å)	EW$_{\rm Ca\ 8662}$ (Å)	EW$_{8542}$/EW$_{8498}$	EW$_{\rm H\alpha}$/EW$_{\rm H\beta}$	EW$_{\rm Li\ I}$ (Å)	Ref.
DX Leo	K0V	6.2	5.38	0.413±0.027	0.274±0.063		0.251±0.028	0.261±0.021	0.377±0.034	0.339±0.030	1.444±0.014		0.183±0.003	[1]
EP Eri	K1V	8.2	6.85				0.171±0.019	0.209±0.019	0.299±0.037	0.252±0.023	1.431±0.047		0.207±0.006	[1]
GJ 211	K1V	4	10.9	–			0.031±0.006	0.125±0.010	0.148±0.014	0.143±0.008	1.184±0.017		0.009±0.002	[1]
HD 166	K0V	6.54	5.69			–	0.055±0.020	0.165±0.100	0.200±0.130		1.212±0.053		0.076±0.001	[1]
BD+174799	K0V	11.03	0.61			0.170±0.006	0.613±0.068	0.375±0.043	0.510±0.073	0.450±0.043	1.360±0.039	3.588±0.273	0.248±0.002	[1]
BD+17232	K4V	20.4	–	0.014±0.03	0.026 ±0.04	0.810±0.017	1.87 ±0.23	–	–	–	–	2.309±0.236	0.406±0.009	[1]
HD 21845	K1V		1.45	–	–	–	0.34 ±0.004	0.27 ±0.04	0.48 ±0.06	–	1.778±0.041		0.220±0.001	[1]
HD 25665	K3V	10.6	–	–	–	–	–	–	–	–	–		0.005±0.001	[1]
GJ 211	K1V	8.69	10.0	–	–	–	0.04 ±0.03	0.12 ±0.04	0.18 ±0.06	0.12 ±0.04	1.500±0.000		0.002±0.001	[1]
BD+201790	K5V	10.03	–	0.075±0.04	0.098 ±0.03	0.878±0.007	1.76 ±0.12	0.54 ±0.06	–	–	–	2.005±0.121	0.085±0.004	[1]
HIP 39721	K5V	0.60	–	–	–	–	–	0.05 ±0.03	0.05 ±0.03	–	1.000±1.00		–	[1]
GJ 9251B	K7V	1.40	–	–	–	–	0.02 ±0.01	0.05 ±0.02	0.05 ±0.01	0.04 ±0.03	1.000±0.20		–	[1]
HIP39896	K7V	11.35	–	0.045±0.03	0.07±0.02	0.655±0.060	1.44 ±0.09	0.431±0.03	0.63 ±0.05	0.46 ±0.07	1.462±0.014	2.198±0.064	–	[1]
HIP 50156	K7V	7.68	7.98	0.06 ±0.02	0.09±0.02	0.795±0.110	1.82 ±0.13	0.40 ±0.05	0.56 ±0.07	0.44 ±0.06	1.400±0.70	2.289±0.153	–	[1]
HD 98736	K1V	1.25	–	–	–	–	–	–	–	–	–		0.015±0.002	[1]
GJ426B	K7V	3.47	–	–	–	–	–	–	–	–	–		0.009±0.002	[1]
HD 112733	K0V	3.11	–	–	–	–	–	–	–	–	–		0.094±0.002	[1]
HD 147379	K7V	9.69	–	–	–	–	0.02 ±0.03	0.04 ±0.02	0.08 ±0.01	0.12 ±0.09	2.000±0.750		–	[1]
HD 160934	K7V	19.73	1.84	0.083±0.03	0.12±0.03	0.840±0.103	1.94 ±0.10	0.49 ±0.08	0.78 ±0.08	0.57 ±0.05	1.592±0.097	2.310±0.164	0.004±0.003	[1]
HIP 87768	K5V	6.92	–	–	–	–	0.03 ±0.03	0.03 ±0.02	0.04 ±0.01	0.03 ±0.01	1.333±0.556		–	[1]
HIP 89874	K5V	20.08	5.15	0.24 ±0.07	0.27±0.09	1.055±0.200	5.17 ±0.39	0.92 ±0.18	1.89 ±0.22	1.49 ±0.19	2.054±0.163	4.900±0.559	0.555±0.017	[1]
HIP 101262	K4V	9.79	–	–	–	–	0.06 ±0.03	0.17 ±0.04	0.15 ±0.06	0.13 ±0.08	0.880±0.145		–	[1]
HIP 106231	K3V	73.52	0.42	0.14 ±0.06	0.18±0.07	0.748±0.115	1.70 ±0.11	0.61 ±0.20	0.78 ±0.20	0.61 ±0.18	–	2.273±0.202	0.233±0.002	[1]
PW And	K2V	23.4	1.75	0.142±0.023	0.117±0.018	0.546±0.068	1.346±0.001	0.506±0.068	0.716±0.076	0.582±0.065	1.415±0.040	2.505±0.126	0.268±0.002	[2,4]
V383 Lac	K1V	19.8	2.42	0.296±0.015	0.213±0.023	0.234±0.049	0.635±0.053	0.415±0.046	0.587±0.060	0.477±0.041	1.414±0.012	2.979±0.314	0.261±0.002	[3,4]
V368 Cep	K1V	16.1	2.74	0.109±0.006	0.070±0.005	0.275±0.070	0.822±0.056	0.399±0.044	0.535±0.064	0.485±0.036	1.341±0.013	2.790±0.36	0.219±0.002	[4]

Ref.: [1] López-Santiago et al. (2010); [2]Montes et al. (2001a); [3] Biazzo et al. (2009); [4] this paper. "–" No emission is detected.

Table 6 Parameters of the linear fits to the maximum amplitudes of chromospheric rotational modulation in the Hα line, and the EWs of the Li 6708 line with stellar $v \sin i$ velocity

Spectral line	EW $= a + b * v \sin i$ velocity		
	a	b	Squared residual
Li I 6708	–0.029±0.049	0.017±0.004	0.525
Maximum amplitude of Hα	0.31 ±0.16	0.014±0.012	1.953

Table 7 Parameters Describing the Linear Fits of EW - $v \sin i$ velocity Relations

Spectral line	EW $= a + b * v \sin i$ velocity		
	a	b	Squared residual
Hα	–0.228 ±0.052	0.067±0.002	0.980
Ca II 8498	0.016 ±0.070	0.027±0.006	0.543
Ca II 8542	–0.072 ±0.144	0.048±0.012	0.484
Ca II 8662	–0.055 ±0.137	0.038±0.011	0.447
EW_{8542}/EW_{8498}	1.142 ±0.120	0.023±0.010	0.223

6.2 GJ 211

GJ 211 is a slowly rotating star (Gaidos et al. 2000; etc). It has shown chromospheric emission in the Ca II H & K lines (Soderblom & Clements 1987), coronal activity (Hünsch et al. 1999) and a flare event (Gershberg et al. 1999). Montes et al. (2000) observed a small excess chromospheric emission in the Ca II H & K lines, the Balmer lines and Ca II IRT lines. All our spectra confirmed the previous results (Figs. 6, 9 and 10). GJ 211 has been measured to have a very small EW (Li I) of 2.0 mÅ (Montes et al. 2001a) and 1.32 mÅ as derived by Gaidos et al. (2000). Our result is 9 ± 2 mÅ, and these indicate that it might not be a member of the Local Association moving group (Montes et al. 2001a).

6.3 The Relation between Chromospheric Activity and Stellar Rotation

As the excess chromospheric emissions vary with phase (Catalano et al. 2002; Biazzo et al. 2007; Frasca et al. 2008a; etc), if we want to obtain the precise relations between chromospheric activity and stellar rotation, we should use the average value of the excess chromospheric emission. We collected the available data on single stars (Biazzo et al. 2009; López-Santiago et al. 2010; Montes et al. 2001a; etc) and calculated their average values (Table 5), which are shown in Figure 12. For the Ca II IRT data, there is a clear trend of increasing the excess chromospheric emission with increasing stellar rotation. The scatter is quite large for the Hα line. It seems that there is a very weak linear relation between Hα and $v \sin i$. The Hα line might be affected by a prominence or chromospheric emission. More data are needed to confirm this. As can be seen from Figure 12, the linear fits demonstrate the trend. The parameters describing the linear fits of the EW-rotation relations are listed in Table 7. All these are consistent with the chromospheric activity-rotation dependence derived by Montes et al. (2001a) and López-Santiago et al. (2005).

Until now, no other authors have discussed the maximum amplitudes of chromospheric rotational modulation with stellar rotation. The maximum amplitude of chromospheric rotational modulation equals the largest EW shown by chromospheric active emission minus the lowest value of chromospheric emission (the quiet chromosphere). They represent variability in chromospheric activity (active chromospheric region). Therefore, we determined the values of the maximum amplitudes of chromospheric rotational modulation for our objects by using the Hα line. To examine the relation between the maximum and $v \sin i$, we also collected the maximum amplitudes for other late-type stars. We listed these values in Table 8. It seems that there might be a trend of increasing activity with increasing $v \sin i$ velocity (Fig. 13). The linear parameters are listed in Table 6. They

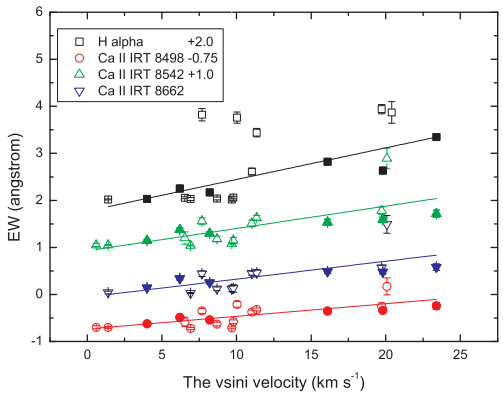

Fig. 12 The values of the Hα, and Ca II IRT excess EWs vs. stellar $v \sin i$ velocity. The different open/colored points represent the previously published data. The solid points represent our data and the solid lines refer to a linear fit to the data.

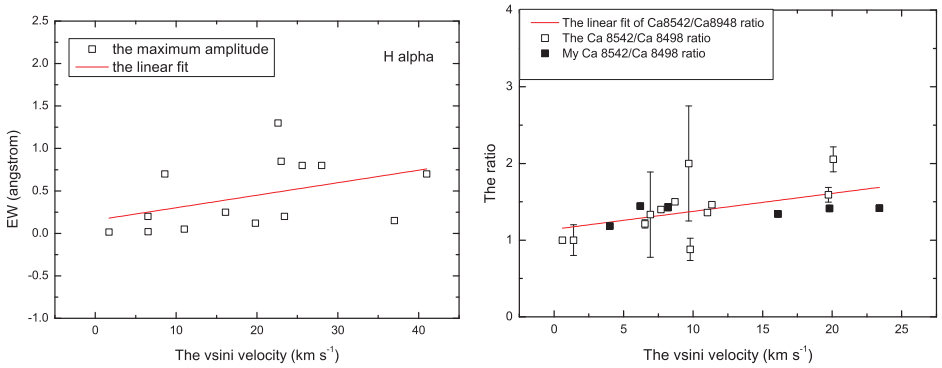

Fig. 13 The maximum amplitudes of chromospheric rotational modulation vs. $v \sin i$ velocity in the Hα line (*left*), and the EW_{8542}/EW_{8498} ratio vs. the $v \sin i$ velocity (*right*). The open points represent the previously published data. The solid points represent our data and the solid line is the linear fit.

Table 8 Maximum Amplitudes of Chromospheric Rotational Modulations for the Late-Type Stars in the Hα Line

Object	Spectral type	$v \sin i$ velocity (km s^{-1})	Period (d)	Max. amplitudes (Å) Hα	Reference
PW And	K2V	23.4	1.75	0.20	López-Santiago et al. (2003)
V383 Lac	K1V	19.8	2.42	0.12	Biazzo et al. (2009)
VY Ari	K0IV	8.6	16.292	0.7	Biazzo et al. (2006)
IM Peg	K2III	25.6	24.789	0.8	Biazzo et al. (2006)
HK Lac	K0III	23	24.283	0.85	Biazzo et al. (2006)
HD17488(V889 Her)	G0V	37	1.337	0.15	Frasca et al. (2010)
II Peg	K2V-IV	22.6	6.7	1.3	Frasca et al. (2008a)
lamb And	G8IV-III	6.5	20.5	0.2	Frasca et al. (2008a)
HD 206860	G0V	11	4.74	0.05	Frasca et al. (2000b)
V711 Tau	K1IV/G5V	41	2.84	0.7	García-Alvarez et al. (2003)
LQ Hya	K2V	28	1.6	0.3	Frasca et al. (2008b)
HD 22049	K2V	1.7	11.7	0.015	Biazzo et al. (2007)
HD 166	K0V	6.54	6.23	0.02	Biazzo et al. (2007)

are consistent with the trend in the photosphere resulting from the maximum amplitudes of spot-induced brightness variations in late-type stars by Messina et al. (2003) and short-period RS CVn binaries (Zhang 2012).

The ratio EW_{8542}/EW_{8498} can be used to differentiate plages from prominences. Until now, no other authors have discussed the relation between the EW_{8542}/EW_{8498} ratio and rotation. We found that there was a weak trend that showed increasing ratios of EW_{8542}/EW_{8498} with increasing $v \sin i$ velocity. The linear fit is shown in Figure 13 and the corresponding result is listed in Table 8. This fit might give us a hint about the relation between the occurrence of a plage (or prominence) and the $v \sin i$ velocity. More theories will be needed to address these topics in the future.

Acknowledgements We are very grateful to Drs. Gu S. H., Cao D. T. and Fang X. S. for their kind help. We would also like to thank Dr. S. C. Barden for developing the STARMOD program. This work was partly supported by the Chinese Academy of Sciences (Grant Nos. 10978010 and U1431114), and by the National Natural Science Foundation of China (Grant Nos. 11263001 and 10373023). This work was supported by the Natural Science Foundation of the Guizhou Province Office of Education (Grant No. 2014298). This work was partially supported by the Open Project Program of the Key Laboratory of Optical Astronomy, NAOC, CAS.

References

Andretta, V., Doyle, J. G., & Byrne, P. B. 1997, A&A, 322, 266
Baliunas, S. L., Donahue, R. A., Soon, W. H., et al. 1995, ApJ, 438, 269
Baliunas, S., Sokoloff, D., & Soon, W. 1996, ApJ, 457, L99
Barden, S. C. 1985, ApJ, 295, 162
Basri, G., Wilcots, E., & Stout, N. 1989, PASP, 101, 528
Berdyugina, S. V. 2005, Living Reviews in Solar Physics, 2, 8
Bianchi, L., Jurcsik, J., & Fekel, F. C. 1991, A&A, 245, 604
Biazzo, K., Frasca, A., Catalano, S., & Marilli, E. 2006, A&A, 446, 1129
Biazzo, K., Frasca, A., Henry, G. W., Catalano, S., & Marilli, E. 2007, ApJ, 656, 474
Biazzo, K., Frasca, A., Marilli, E., et al. 2009, A&A, 499, 579
Bidelman, W. P. 1985, AJ, 90, 341
Bowyer, S., Lieu, R., Lampton, M., et al. 1994, ApJS, 93, 569
Bouvier, J., Wichmann, R., Grankin, K., et al. 1997, A&A, 318, 495
Buzasi, D. L. 1989, A study of active regions on RS CVn stars, Ph.D. Thesis, Pennsylvania State University, University Park
Cao, D.-T., & Gu, S.-H. 2012, A&A, 538, A130
Catalano, S., Biazzo, K., Frasca, A., & Marilli, E. 2002, A&A, 394, 1009
Cayrel de Strobel, G., & Cayrel, R. 1989, A&A, 218, L9
Chester, M. M. 1991, Testing the solar paradigm for chromospheric activity in RS CVN binaries: Moderate resolution spectroscopy of solar active regions, Ph.D. Thesis, Pennsylvania State University, University Park
Christian, D. J., Craig, N., Dupuis, J., Roberts, B. A., & Malina, R. F. 2001, AJ, 122, 378
Cutispoto, G. 1992, A&AS, 95, 397
Eker, Z., Hall, D. S., & Anderson, C. M. 1995, ApJS, 96, 581
Eker, Z., Ak, N. F., Bilir, S., et al. 2008, MNRAS, 389, 1722
Favata, F., Barbera, M., Micela, G., & Sciortino, S. 1995, A&A, 295, 147
Fekel, F. C., Bopp, B. W., Africano, J. L., et al. 1986, AJ, 92, 1150
Fekel, F. C. 1997, PASP, 109, 514
Fraquelli, D. A. 1984, ApJ, 276, 243
Frasca, A., Freire Ferrero, R., Marilli, E., & Catalano, S. 2000a, A&A, 364, 179

Frasca, A., Marino, G., Catalano, S., & Marilli, E. 2000b, A&A, 358, 1007
Frasca, A., Çakırlı, Ö., Catalano, S., et al. 2002, A&A, 388, 298
Frasca, A., Biazzo, K., Taş, G., Evren, S., & Lanzafame, A. C. 2008a, A&A, 479, 557
Frasca, A., Kovári, Z., Strassmeier, K. G., & Biazzo, K. 2008b, A&A, 481, 229
Frasca, A., Biazzo, K., Kővári, Z., Marilli, E., & Çakırlı, Ö. 2010, A&A, 518, A48
Gaidos, E. J., Henry, G. W., & Henry, S. M. 2000, AJ, 120, 1006
Gálvez, M. C., Montes, D., Fernández-Figueroa, M. J., De Castro, E., & Cornide, M. 2009, AJ, 137, 3965
García-Alvarez, D., Foing, B. H., Montes, D., et al. 2003, A&A, 397, 285
Gershberg, R. E., Katsova, M. M., Lovkaya, M. N., Terebizh, A. V., & Shakhovskaya, N. I. 1999, A&AS, 139, 555
Griffin, R. E. M., & Griffin, R. F. 2004, MNRAS, 350, 685
Gu, S.-h., Collier Cameron, A., & Kim, K. M. 2010, in IAU Symposium, 264, eds. A. G. Kosovichev, A. H. Andrei, & J.-P. Rozelot, 90
Gu, S.-H., Tan, H.-S., Shan, H.-G., & Zhang, F.-H. 2002, A&A, 388, 889
Güdel, M. 2002, ARA&A, 40, 217
Gunn, A. G., & Doyle, J. G. 1997, A&A, 318, 60
Hall, J. C. 2008, Living Reviews in Solar Physics, 5, 2
Hall, J. C., & Ramsey, L. W. 1992, AJ, 104, 1942
Henry, G. W., Eaton, J. A., Hamer, J., & Hall, D. S. 1995a, ApJS, 97, 513
Henry, G. W., Fekel, F. C., & Hall, D. S. 1995b, AJ, 110, 2926
Herbig, G. H. 1985, ApJ, 289, 269
Høg, E., Fabricius, C., Makarov, V. V., et al. 2000, A&A, 355, L27
Hooten, J. T., & Hall, D. S. 1990, ApJS, 74, 225
Houdebine, E. R., Stempels, H. C., & Oliveira, J. H. 2009, MNRAS, 400, 238
Hünsch, M., Schmitt, J. H. M. M., Sterzik, M. F., & Voges, W. 1999, A&AS, 135, 319
Jeffries, R. D. 1995, MNRAS, 273, 559
Joy, A. H., & Wilson, R. E. 1949, ApJ, 109, 231
Kahanpää, J., Jetsu, L., Alha, L., et al. 1999, A&A, 350, 513
Kashapova, L. K., Kotrč, P., & Kupryakov, Y. A. 2008, Annales Geophysicae, 26, 2975
Lazaro, C., & Arevalo, M. J. 1997, AJ, 113, 2283
López-Santiago, J., Montes, D., Fernández-Figueroa, M. J., & Ramsey, L. W. 2003, A&A, 411, 489
López-Santiago, J., Montes, D., Fernández-Figueroa, M. J., Gálvez, M. C., & Crespo-Chacón, I. 2005, in ESA Special Publication, 560, 13th Cambridge Workshop on Cool Stars, Stellar Systems and the Sun, eds. F. Favata, G. A. J. Hussain, & B. Battrick, 775
López-Santiago, J., Montes, D., Crespo-Chacón, I., & Fernández-Figueroa, M. J. 2006, ApJ, 643, 1160
López-Santiago, J., Montes, D., Gálvez-Ortiz, M. C., et al. 2010, A&A, 514, A97
Mantegazza, L., Poretti, E., Antonello, E., & Bossi, M. 1992, A&A, 256, 459
Martínez-Arnáiz, R., López-Santiago, J., Crespo-Chacón, I., & Montes, D. 2011, MNRAS, 414, 2629
Messina, S., & Guinan, E. F. 1996, Information Bulletin on Variable Stars, 4286, 1
Messina, S., Guinan, E. F., Lanza, A. F., & Ambruster, C. 1999, A&A, 347, 249
Messina, S., Pizzolato, N., Guinan, E. F., & Rodonò, M. 2003, A&A, 410, 671
Montes, D., Fernandez-Figueroa, M. J., de Castro, E., & Cornide, M. 1995, A&A, 294, 165
Montes, D., Fernandez-Figueroa, M. J., de Castro, E., & Sanz-Forcada, J. 1997, A&AS, 125, 263
Montes, D., Saar, S. H., Collier Cameron, A., & Unruh, Y. C. 1999, MNRAS, 305, 45
Montes, D., Fernández-Figueroa, M. J., De Castro, E., et al. 2000, A&AS, 146, 103
Montes, D., López-Santiago, J., Fernández-Figueroa, M. J., & Gálvez, M. C. 2001a, A&A, 379, 976
Montes, D., López-Santiago, J., Gálvez, M. C., et al. 2001b, MNRAS, 328, 45
Montes, D., Crespo-Chacón, I., Gálvez, M. C., et al. 2004, Lecture Notes and Essays in Astrophysics, 1, 119

Mulliss, C. L., & Bopp, B. W. 1994, PASP, 106, 822
Nugent, J. J., Jensen, K. A., Nousek, J. A., et al. 1983, ApJS, 51, 1
Osten, R. A., & Saar, S. H. 1998, MNRAS, 295, 257
Pandey, J. C., & Singh, K. P. 2008, MNRAS, 387, 1627
Pasquini, L., Pallavicini, R., & Pakull, M. 1988, A&A, 191, 253
Piau, L., & Turck-Chièze, S. 2002, ApJ, 566, 419
Poretti, E., Mantegazza, L., & Antonello, E. 1985, Information Bulletin on Variable Stars, 2807, 1
Pounds, K. A., Abbey, A. F., Barstow, M. A., et al. 1991, MNRAS, 253, 364
Pravdo, S. H., White, N. E., & Giommi, P. 1985, MNRAS, 215, 11
Pye, J. P., McGale, P. A., Allan, D. J., et al. 1995, MNRAS, 274, 1165
Rebolo, R., & Beckman, J. E. 1988, A&A, 201, 267
Robb, R. M., Steinbring, E., Balogh, M., et al. 1995, Information Bulletin on Variable Stars, 4281, 1
Shcherbakov, A. G., Shcherbakova, Z. A., Tuominen, I., & Jetsu, L. 1996, A&A, 309, 655
Soderblom, D. R., & Clements, S. D. 1987, AJ, 93, 920
Soderblom, D. R., Pilachowski, C. A., Fedele, S. B., & Jones, B. F. 1993a, AJ, 105, 2299
Soderblom, D. R., Stauffer, J. R., Hudon, J. D., & Jones, B. F. 1993b, ApJS, 85, 315
Strassmeier, K. G., Hall, D. S., Fekel, F. C., & Scheck, M. 1993, A&AS, 100, 173
Strassmeier, K. G., Bartus, J., Cutispoto, G., & Rodono, M. 1997, A&AS, 125, 11
Strassmeier, K., Washuettl, A., Granzer, T., Scheck, M., & Weber, M. 2000, A&AS, 142, 275
Strassmeier, K. G., & Rice, J. B. 2006, A&A, 460, 751
Strassmeier, K. G. 2009, A&A Rev., 17, 251
Tschäpe, R., & Rüdiger, G. 2001, A&A, 377, 84
Wang, H. J., Wei, J. Y., Shi, J. R., & Zhao, J. K. 2009, A&A, 500, 1215
Wichmann, R., Schmitt, J. H. M. M., & Hubrig, S. 2003, A&A, 399, 983
Wood, B. E., Ambruster, C. W., Brown, A., & Linsky, J. L. 2000, ApJ, 542, 411
Xing, L.-F., Shi, J.-R., & Wei, J.-Y. 2007a, New Astron., 12, 265
Xing, L.-F., Zhao, S.-Y., Su, W., et al. 2007b, ChJAA (Chin. J. Astron. Astrophys.), 7, 551
Zhang, L.-Y., & Gu, S.-H. 2008, A&A, 487, 709
Zhang, L. 2011, in Astronomical Society of the Pacific Conference Series, 451, eds. S. Qain, K. Leung, L. Zhu, & S. Kwok, 123
Zhang, L.-Y. 2012, RAA (Research in Astronomy and Astrophysics), 12, 433
Zhang, L., Pi, Q., Zhu, Z., Zhang, X., & Li, Z. 2014, New Astron., 32, 1
Zhao, G., & Li, H.-B. 2001, ChJAA (Chin. J. Astron. Astrophys.), 1, 555
Zhao, J. K., Oswalt, T. D., Rudkin, M., Zhao, G., & Chen, Y. Q. 2011, AJ, 141, 107
Zhao, J. K., Oswalt, T. D., Zhao, G., et al. 2013, AJ, 145, 140
Zirin, H. 1988, Astrophysics of the Sun (Cambridge: Cambridge University Press)